

CHAPTER V

DEVELOPMENTS IN HYBRID COMPARATORS TO YIELD CONIC CHARACTERISTICS

5.1 INTRODUCTION :

The possible applications of conic characteristics are well known and an elliptical characteristic could be preferred over a mho characteristic for the protection of long lines as the former fits more snugly round the fault area. For the blocking of relays during power swings blinder characteristics in the form of two parallel straight lines are generally employed which could be replaced by the conic characteristics like hyperbola or parabola³⁸.

An elliptical characteristic was first obtained by Bräten and Hoël employing multi-input amplitude comparator in the form of a circulating current bridge⁹. However, the relay was not instantaneous in operation due to the requirement of a sensitive polarised moving iron or moving coil type output relay. Skuderna subsequently reported the mathematical basis of conic relays alongwith the necessary circuitry to be used in conjunction with electro-mechanical relays⁴⁹. The hybrid comparator reported by Parthasarathy although yielded all conic pick-up characteristics, however, was slow in operation due to the necessity of sensitive polarised averaging relay in the output stage⁴¹. Further, the circuitry needed a standard

reference for balancing purpose.

An attempt has been made in this chapter to develop a new hybrid comparator to yield conic pick-up characteristics avoiding the use of averaging out-put relay so as to make possible the use of thyristor in the output stage rendering the relay completely static and fast in operation. This comparator incidently forms the basis for the development of a relay with a self-adjusting feature (discussed in the subsequent chapter) .

5.2 PRINCIPLE OF OPERATION :

Fig.5.1 shows the comparator in block-schematic form. System quantities V_L and I_L are applied to the measuring circuits (M) which produce the required unmixed signals S_1 and S_2 for the phase comparison and S_K for the d.c. biasing of the phase comparator (P.C.) after rectification and adequate filtering(R.F.). Further, the measuring circuits provide the signals S_A and S_B which are required as polarising inputs to the Amplitude comparator of the output stage(O.S.) after rectification and filtering.

The output of the phase comparator is a square-wave of positive duration equal to the negative coincidence of S_1 and S_2 . This square-wave is used to generate a function e_c , by means of the function generator(F.G.), given by

$$e_c = K_1 | S_K | (1 - \cos \delta) \quad \dots \quad (5.1)$$

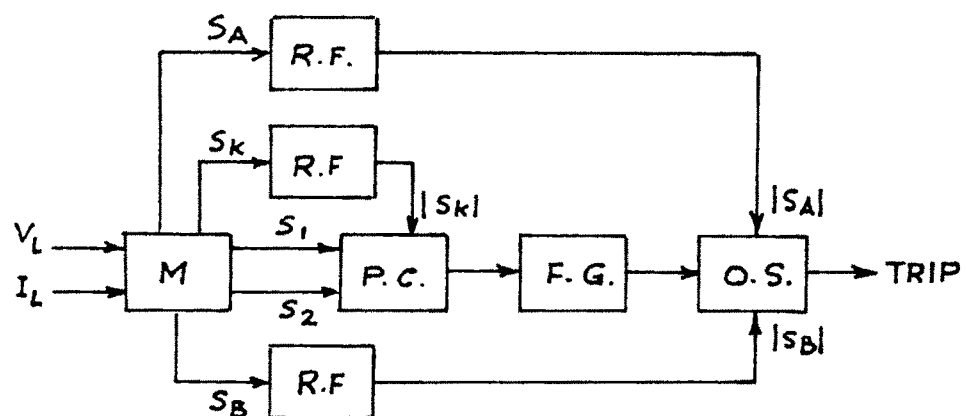


FIG. 5-1 BLOCK-SCHIMATIC DIAGRAM OF THE
COMPARATOR

where, K_1 is a constant. $|S_K|$ is the derived system quantity and γ is the negative coincidence period of S_1 and S_2 , which in fact depends on θ and ϕ , θ being the angle of replica impedance introduced in the measuring circuits.

Comparison of the function of Eq.(5.1) with the derived system quantities $|S_A|$ and $|S_B|$ for the amplitude is the basis of obtaining various conic characteristics.

5.3 MATHEMATICAL BASIS :

In view of the above principle of operation the necessary mathematical basis will now be developed for various conic characteristics.

5.3.1 Ellipse :

To obtain this characteristic on the impedance plane the necessary inputs to the phase comparator are ,

$$\begin{aligned} S_1 &= I_L Z_R \angle \theta - \phi \\ \text{and } S_2 &= -V_L \end{aligned} \quad \begin{array}{c} 0 \\ 0 \\ 0 \\ 0 \end{array} \quad \dots (5.2)$$

Where $Z_R \angle \theta$ is the replica impedance introduced in the measuring circuits.

On choosing $|S_K| = |S_2|$, eq.(5.1) becomes

$$e_c = K_1 |V_L| [1 - \cos(\theta - \phi)] \quad \dots (5.3)$$

Voltage, e_c of (5.3) is to be compared with $|S_A| = K_2 |I_L Z_R|$ and $|S_B| = K_3 |V_L|$ in the amplitude comparator such that the latter issues a tripping signal when,

$$K_1 |V_L| [1 - \cos(\theta - \phi)] \leq K_2 |I_L Z_R| - K_3 |V_L| \dots (5.4)$$

where, K_2 and K_3 are real constants less than or equal to 1, in most of the cases representing the potentiometer settings.

Inequality (5.4) can be written as ,

$$Z_L \leq \frac{K' Z_R}{1 - K'' \cos(\theta - \phi)} \dots (5.5)$$

Where, $Z_L = V_L / I_L$. Further $K' = K_2 / (K_1 + K_3)$ and $K'' = K_1 / (K_1 + K_3)$.

For the values of K'' less than 1, the inequality (5.5) represents the elliptical characteristic of fig.5.2(a). The axes of the ellipse are $2K'Z_R/(1-K''^2)$ and $2K'Z_R/(\sqrt{1-K''^2})$, and the centre is $[K'K''Z_R/(1-K''^2); \theta]$. The semi-latus rectum is $K'Z_R$.

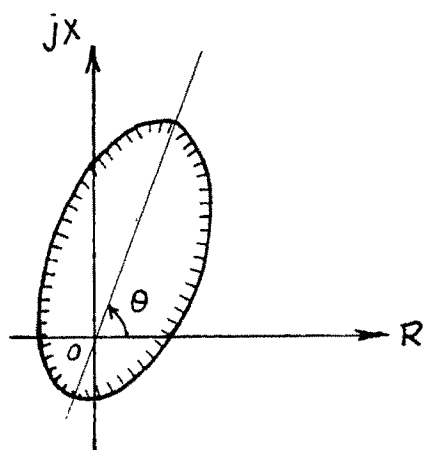
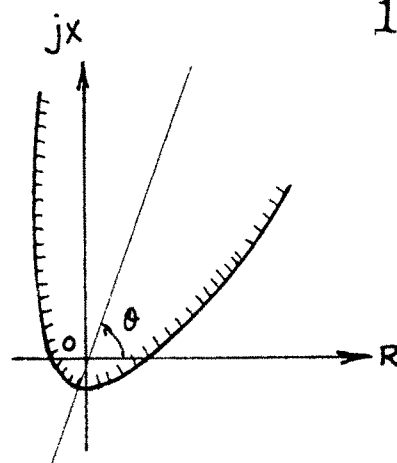
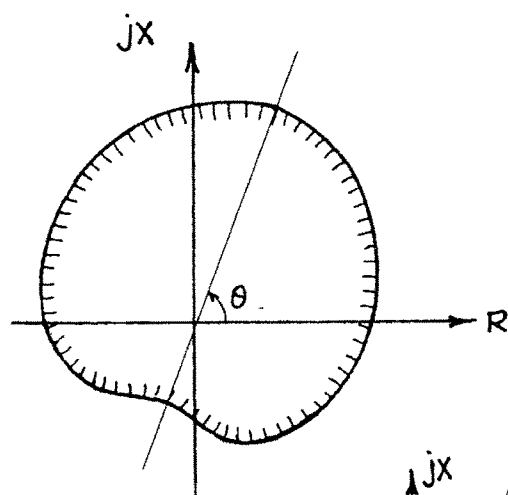
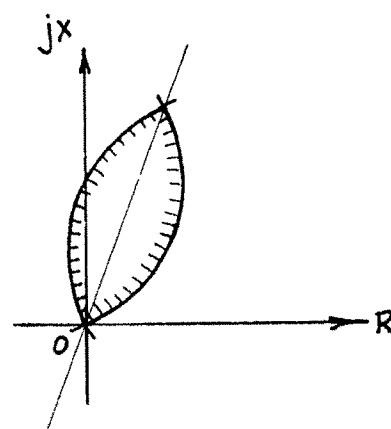
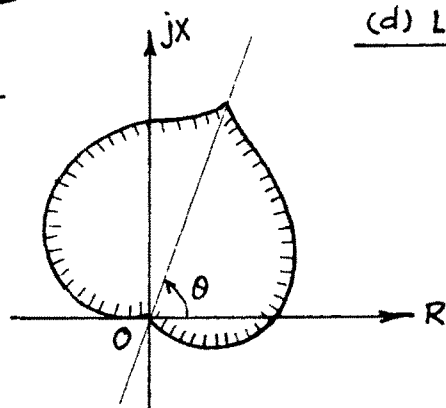
5.3.2 Parabola :

On substituting $K_3=0$ in (5.4) the latter reduces to,

$$K_1 |V_L| [1 - \cos(\theta - \phi)] \leq K_2 |I_L Z_R| \dots (5.6)$$

inequality (5.6) can be further written as

$$Z_L \leq \frac{K' Z_R}{1 - \cos(\theta - \phi)} \dots (5.7)$$

(a) ELLIPSE(b) PARABOLA(c) LIMACON ($a > b$)(d) LIMACON ($a < b$)(e) CARDIOIDFIG. 5-2 CONIC CHARACTERISTICS

where $K_1' = K_2 / K_1$.

Inequality(5.7) represents a parabola on the impedance plane as shown in fig.5.2(b). The axis of the parabola is inclined at θ^0 with the R-axis. The directrix is the line perpendicular to the axis and away from the origin by a distance $K_1' Z_R$.

5.3.3 Limacon :

To obtain this characteristic, the necessary signals for the phase comparison are,

$$\begin{aligned} S_1 &= I_L Z_R \angle \theta - \phi \\ S_2 &= V_L \end{aligned} \quad \begin{array}{c} 0 \\ 0 \\ 0 \\ 0 \end{array} \quad \dots (5.8)$$

On choosing $|S_K| = |S_1|$, (5.1) becomes

$$e_c = K_1 |I_L Z_R| [1 + \cos(\theta - \phi)] \quad \dots (5.9)$$

voltage e_c of (5.9) is to be compared with $|S_A| = K_2 |I_L Z_R|$ and $|S_B| = K_3 |V_L|$ in the amplitude comparator such that the latter issues a tripping signal when,

$$K_1 |I_L Z_R| [1 + \cos(\theta - \phi)] \geq K_3 |V_L| - K_2 |I_L Z_R| \quad \dots (5.10)$$

$$\text{or, } Z_L \leq \frac{Z_R}{K_3} [a + b \cos(\theta - \phi)] \quad \dots (5.11)$$

$$\begin{aligned} \text{where } a &= K_1 + K_2, \text{ and} \\ b &= K_1 \end{aligned} \quad \begin{array}{c} 0 \\ 0 \\ 0 \end{array} \quad \dots (5.12)$$

From (5.12) it is evident that for the positive values of K_1 and K_2 , $a > b$. The inequality (5.11), therefore represents a limaçon which encloses the origin of the impedance plane as shown in fig. 5.2(c). If, however, K_2 is made negative, then, inequality (5.11) will represent a limaçon passing through the origin of the impedance plane [fig. 5.2(d)].

5.3.4 Cardioid :

Cardioid is a special case of limaçon, with $a = b$. Substituting $K_2 = 0$ in (5.10) the latter reduces to

$$K_1 | I_L Z_R | [1 + \cos(\theta - \phi)] \geq K_3 | V_L | \dots (5.13)$$

or

$$Z_L \leq \frac{K_1}{K_3} Z_R [1 + \cos(\theta - \phi)] \dots (5.14)$$

Inequality (5.14) represents a cardioid on the impedance plane [fig. 5.2(e)] whose axes is inclined at θ° with the R-axis. Further, it passes through the points $(0 ; 0)$, $(2K_1 Z_R / K_3 ; \theta)$, $(K_1 Z_R / K_3 ; \theta + 90^\circ)$, and $(K_1 Z_R / K_3 ; \theta - 90^\circ)$.

5.4 RELAY CIRCUITRY FOR ELLIPTICAL CHARACTERISTIC :

The mathematical basis developed in section 5.3.1, together with the principle of operation outlined in section 5.3, will now be used in explaining the complete relay circuitry yielding elliptical characteristic.

5.4.1 The Phase Comparator :

Fig.5.3 shows the phase comparator employed for the phase comparison of S_1 and S_2 given by (5.2). The comparator is supplied with $|V_L|$ for d.c.biassing. It is evident that the comparator will provide square-wave output of approximate magnitude $|V_L|$ and duration $\gamma = (\theta - \phi)$ as shown in fig.5.4 and plates 5.1 and 5.2. This square-wave is used to generate the function of eq.(5.1).

5.4.2 The Function Generator :

The function generating circuit is shown in fig.5.5 which also includes the phase comparator of fig.5.3 for convenience. The square-wave obtained by the phase comparison of S_1 and S_2 is used to charge the capacitor C towards $|V_L|$ with a time constant $(R_3 + R_4)C$. R_3, R_4 and C are so chosen that the charging time constant is large and discharging time constant small so that e_c' , the voltage across the capacitor, shall rise linearly with increasing values of $\lambda = \omega t$ upto a point P and then follow an exponential path as shown in fig.5.6. In the remaining period C will discharge completely.

Alternatively, R_3 may be chosen large with $R_4 = 0$, so that the charging of C will be as above and discharging almost instantaneous as shown by the dotted curve(fig.5.6).

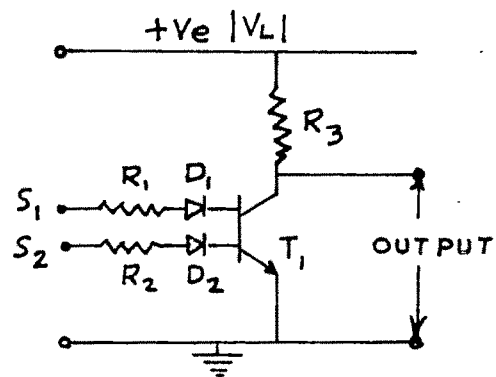


FIG. 5.3 THE PHASE COMPARATOR

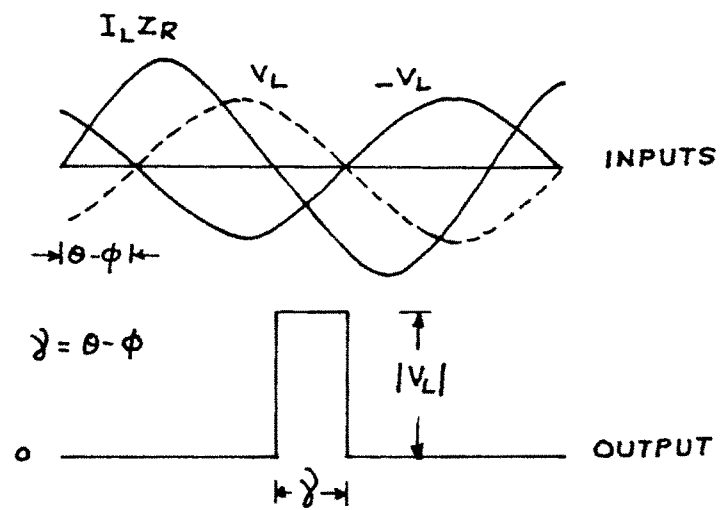


FIG. 5.4 PHASE COMPARISON

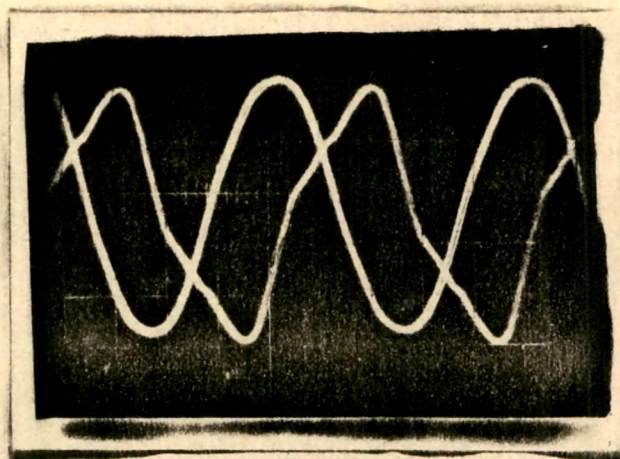


Plate 5.1 Inputs to the phase comparator

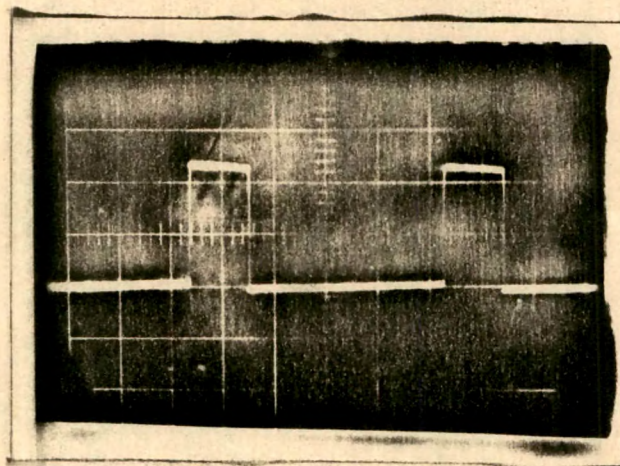


Plate 5.2 Square-wave output of the phase comparator

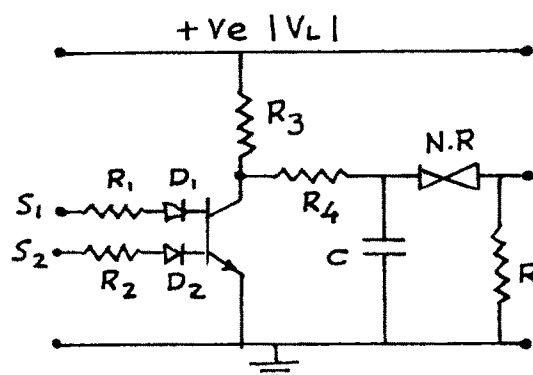


FIG. 5-5 FUNCTION GENERATING CIRCUIT

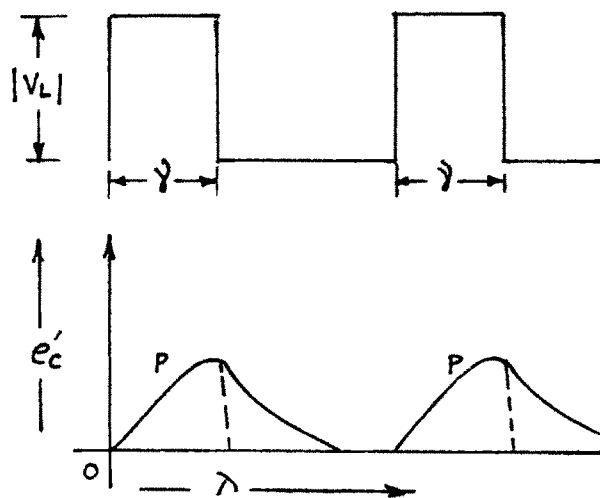


FIG. 5-6 CHARGING OF THE CAPACITOR

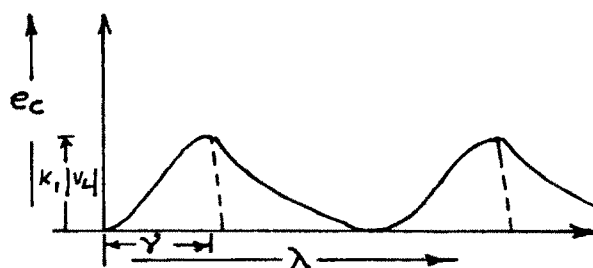


FIG. 5-7 VOLTAGE MODIFIED BY N.R.

The voltage e_c' is applied to the amplitude comparator through the non-linear resistance, N.R. . R is the input resistance of the following circuitry. Due to the application of e_c' the current will flow through the non-linear resistance producing a non-linear voltage drop . e_c , the voltage modified by the non-linear resistance is shown in fig.5.7 .

On choosing proper values of R_3 , R_4 , C and N.R., the rising portion of the curve of fig.5.7 can be approximately written as,

$$e_c = K_1 |V_L| [(1 - \cos \gamma)] \quad \dots (5.15)$$

Since $\gamma = \theta - \phi$ (fig.5.4) , inequality(5.15) becomes

$$e_c = K_1 |V_L| [1 - \cos(\theta - \phi)] \quad \dots (5.16)$$

5.4.3 Rectifying and Filtering Circuits :

For obtaining rectified voltages from S_K , S_A and S_B , full-wave rectifiers followed by filtering circuits are employed. To obtain low ripple in the rectified voltages without sacrificing the time of operation of the relay capacitance multiplier circuits are employed for filtering. Fig.5.8 shows a typical full wave rectifier followed by a capacitance multiplier circuit.

Full-wave rectified voltage is applied to the transistor T connected in common collector mode(more aptly emitter

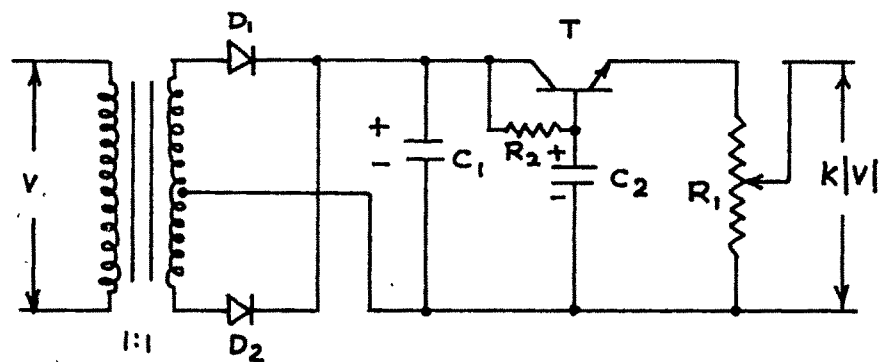


FIG. 5.8 RECTIFIER AND FILTER

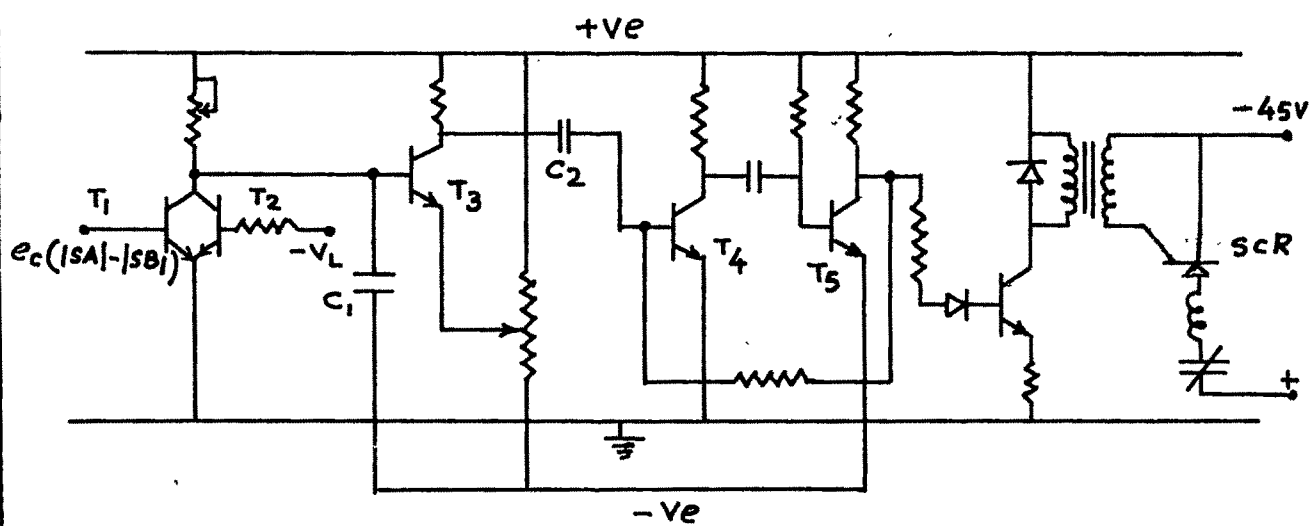


FIG. 5.9 OUTPUT STAGE

follower) through initial filtering due to C_1 . The circuit provides small dynamic time constant with multiplied capacitance for the filtering.

5.4.4 Output Stage :

Signals $K_2|I_L Z_R|$ and $K_3|V_L|$ are obtained from respective signals $I_L Z_R$ and V_L using rectifier and filter circuits of fig.5.8 . $K_3|V_L|$ is subtracted from $K_2|I_L Z_R|$, and the resulting quantity is further subtracted from e_c of equation 5.16 and applied to the output stage which incorporates the amplitude comparator. With this arrangement it is possible to satisfy inequality(5.4) to yield the elliptical characteristic. On the verge of operation of the relay the input to the output stage will be a small pulse corresponding to the peak of the voltage e_c which occurs in the negative half cycle of $-V_L$. To block, therefore, the output of the relay during the positive half cycle of the signal $-V_L$, a typical output stage is arranged as shown in fig.5.9 .

During the positive half cycle of $-V_L$, T_2 conducts providing only a small voltage across the capacitor C_1 corresponding to the drop across T_2 . This voltage, however, is too small to make T_3 conduct which is emitter-biased. There is no input, therefore to the monostable multi-vibrator circuit. The relay, therefore, does not issue a tripping signal.

During the negative half cycle of $-V_L$, T_2 cannot conduct. If the input to the base of T_1 is positive (impedance seen by the relay outside the characteristic), T_1 will conduct. No output, therefore, will appear from the multi-vibrator to trip the circuit breaker. In the event of the inequality (5.4) getting satisfied, both T_1 and T_2 will stop conducting. During this period C_1 will charge towards the d.c. supply and overcome the emitter bias of T_3 . This will result in production of a negative pulse (plate 5.3) which triggers the multi-vibrator circuit. A positive pulse, therefore appears from the output terminals of the multi-vibrator which can be used to trigger a thyristor placed in the trip-circuit of the circuit breaker, rendering the relay completely static and fast in operation.

5.5 PERFORMANCE TESTS :

The relay described in the previous section was constructed and tested during steady-state conditions only. Fig.5.10 shows the complete relay circuit yielding elliptical characteristic. The results obtained during the investigation are presented in Appendix alongwith the necessary testing set up. The circuits were also arranged to provide tripping in accordance with (5.6), (5.10) and (5.13) to yield parabola, limacon and cardioid respectively. The results obtained during the investigation are also presented in the Appendix.

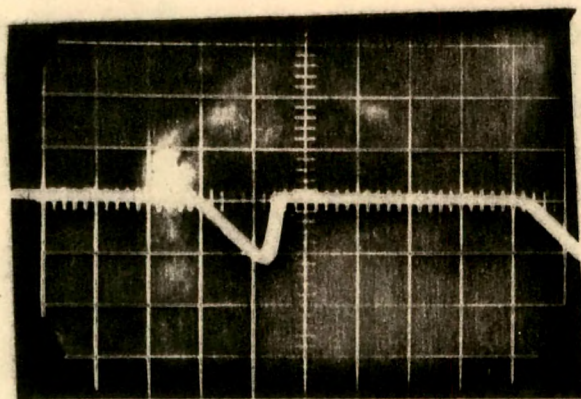


Plate 5.3 Output of the
Transistor T_3

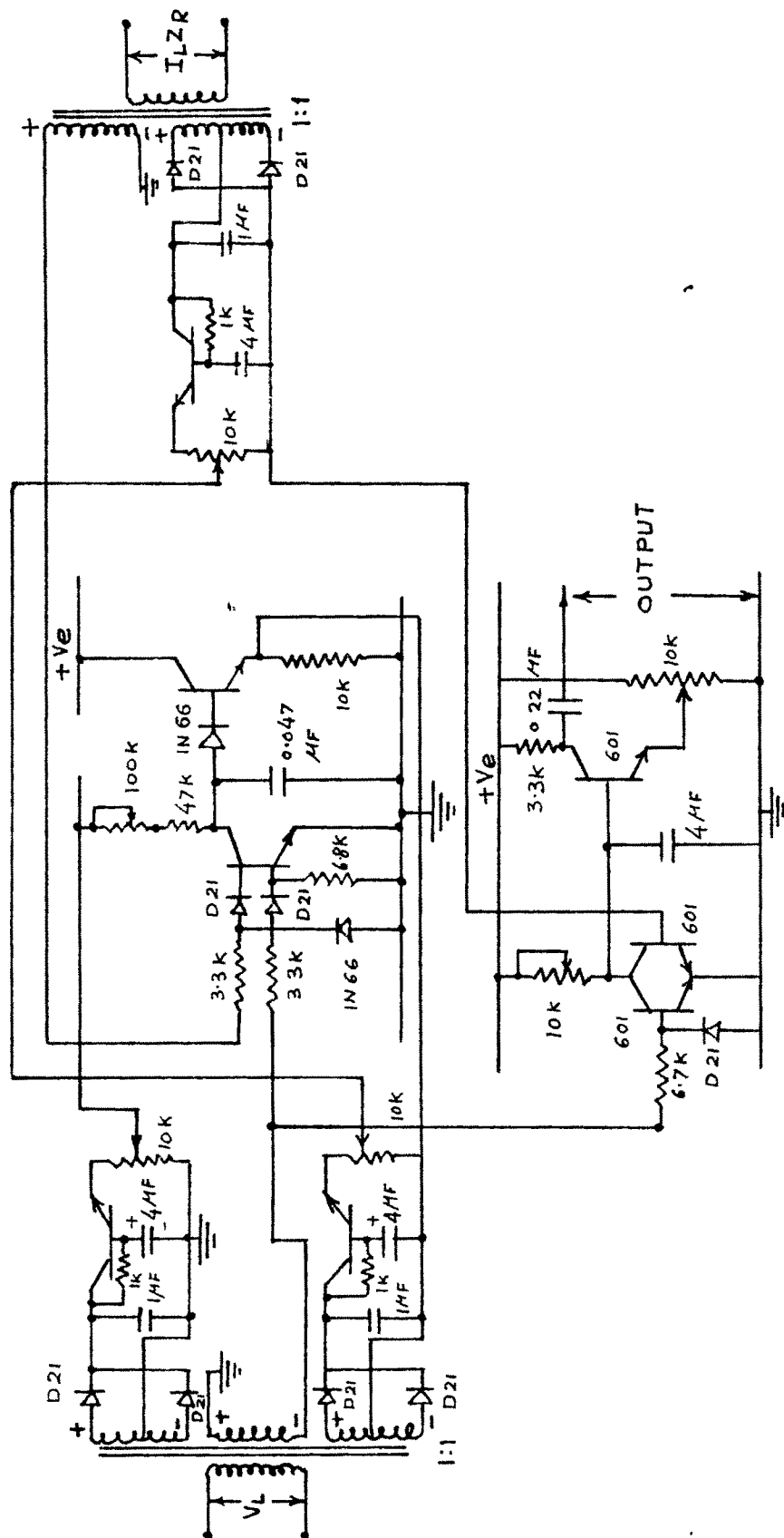


FIG. 5-10 COMPLETE RELAY CIRCUIT FOR ELLIPTICAL CHARACTERISTIC